

## Behavior of stiffened and unstiffened CFT under concentric loading, An experimental study

Ahmed F. Deifalla<sup>1a</sup>, Fattouh M. Fattouh<sup>2b</sup>, Mona M. Fawzy<sup>\*3</sup> and Ibrahim S. Hussein<sup>2c</sup>

<sup>1</sup> Department of Structural Engineering, Faculty of Engineering, Future University in Egypt, End of 90th St., Fifth Settlement, New Cairo, Cairo 11865, Egypt

<sup>2</sup> Department of Structural Engineering, Faculty of Engineering, Helwan University Ain Helwan 11795, Cairo, Egypt

<sup>3</sup> Structural Engineering, Higher Institute of Engineering, El-Shorouk Academy, Nakheel district 11837, Cairo, Egypt

(Received April 6, 2019, Revised October 28, 2019, Accepted November 27, 2019)

**Abstract.** Concrete-filled steel tubular (CFST) beam-columns are widely used owing to their good performance. They have high strength, ductility, large energy absorption capacity and low costs. Externally stiffened CFST beam-columns are not used widely due to insufficient design equations that consider all parameters affecting their behavior. Therefore, effect of various parameters (global, local slenderness ratio and adding hoop stiffeners) on the behavior of CFST columns is studied. An experimental study that includes twenty seven specimens is conducted to determine the effect of those parameters. Load capacities, vertical deflections, vertical strains and horizontal strains are all recorded for every specimen. Ratio between outer diameter (D) of pipes and thickness (t) is chosen to avoid local buckling according to different limits set by codes for the maximum D/t ratio. The study includes two loading methods on composite sections: steel only and steel with concrete. The case of loading on steel only, occurs in the connection zone, while the other load case occurs in steel beam connecting externally with the steel column wall. Two failure mechanisms of CFST columns are observed: yielding and global buckling. At early loading stages, steel wall in composite specimens dilated more than concrete so no full bond was achieved which weakened strength and stiffness of specimens. Adding stiffeners to the specimens increases the ultimate load by up to 25% due to redistribution of stresses between stiffener and steel column wall. Finally, design equations previously prepared are verified and found to be only applicable for medium and long columns.

**Keywords:** steel-concrete; composite columns; experimental study; stiffeners

### 1. Introduction

Recent years have witnessed increasing interest in the use of CFST columns. They are widely used in high rise composite buildings and bridges. They are constructed by filling either normal or high strength concrete into a normal or high strength hollow steel tube. They have many advantages such as high resistance to lateral torsional buckling and torsion.

Extensive research aims to maximize application of CFST columns. Their behavior under axial and flexural loads was investigated by Gupta *et al.* (2007). These studies included various factors for instance: diameter to thickness (D/t) ratio, grade of concrete, tube shape, tube tensile strength, compressive load ratio and column length to diameter (H/D) ratio. Generally previous research of Sakino *et al.* (2004) has proved that the maximum axial load of circular CFST columns is higher than nominal squash load

of concrete and steel separately. The variation in poisson's ratio of concrete and steel governs the behavior of axially loaded circular CFST columns. When lateral deformations increase, tensile hoop stresses appear in steel tube. As a result, confining effects and triaxial compressive stresses occurs in the concrete core causing increased axial load capacity of circular CFT columns.

Method of loading of CFST columns carried out by Hajar (2000) where applying load on concrete only, showed confinement effects at low loading levels. On the other hand, loading the steel section only causes friction at the connection vicinity while confinement effects are not noticeable until loading is transferred to the concrete core. Fam *et al.* (2004) applied axial load on concrete core only and on composite section of steel and concrete beam columns under lateral loads. The bond and end loading conditions had no effect on flexural strength of members.

Properties of materials affect the behavior of CFST elements under axial or flexural loading. The effect of using high strength steel and/or concrete has been investigated. Sixty five specimens under eccentric loads are tested. Nishiyama and Morino (2004) reported that moment curvature relationships for circular columns are stable with large ductility. The moment curvature relationship of a circular CFT column is highly affected by the stress strain relationship of concrete better than the stress strain relation of steel tube. On the other hand, using high strength

\*Corresponding author, Assistant Professor,  
E-mail: [m.fawzy@sha.edu.eg](mailto:m.fawzy@sha.edu.eg)

<sup>a</sup> Associate Professor

<sup>b</sup> Associate Professor

<sup>c</sup> Ph.D. Researcher, Ph.D. Student,  
E-mail: [eng.elsayed.ebrahim@sha.edu.eg](mailto:eng.elsayed.ebrahim@sha.edu.eg)

concrete with low strength steel tubes is not recommended. The effect of confinement is not influential in that case, while the local buckling becomes clear.

The failure mode of CFST columns sections is affected by H/D ratio and width to thickness (w/t) ratios. According to Hajjar *et al.* (1998) CFST columns with H/D ratio below approximately 10-15 and under monotonic loading will fail near their cross section strength. Slender CFST columns have flexural instability which prevents the section from reaching its maximum capacity. Their failure occurs by a combination of yielding of steel, local buckling of steel, crushing of concrete and flexural buckling of the member. Failure of thin walled steel tubes occurs by local buckling of steel and shear failure of concrete. Hu *et al.* (2003) reported that the circular steel tube can provide a confining behavior to concrete when D/t is less than 40. Failure of the thin CFST columns with D/t ratio more than 60 usually fails by local buckling of the steel tube combined with shear failure of concrete.

Ajel and Abbas (2015) studied the behavior of stiffened CFST columns using experimental tests and analytical study. The effect of concrete compressive strength, thickness of steel tube, internal stiffeners and longitudinal reinforcement were considered. Specimens that were studied consisted of sixteen square samples. The tested samples were also studied analytically using three dimensional finite element representation by ANSYS (ver. 12.1) computer program. Parametric studies regarding number of transversely stiffened I-section plate girders. The ratio of width-thickness and diameter/thickness were inversely proportional to the ultimate strength of columns. The increase in ultimate load of columns varied from 4% to 13 % for square samples, while varied from 8% to 12% for circular samples depending on the type of stiffeners, compressive strength of concrete and ratios of width-thickness and diameter/thickness. Patel (2013) prepared numerical models for nonlinear inelastic analysis of thin-walled rectangular and circular slender steel concrete filled beam-columns. Parameters discussed are concrete confinement, geometric imperfections, preloads, high strength materials, second order and cyclic behavior. The most important conclusions were that cyclic local buckling considerably reduces the ultimate cyclic lateral loads and ductility of specimens. The use of high strength concrete did not show a significant increase in the ultimate cyclic lateral loads of concrete filled steel tube slender beam-columns. Petrus *et al.* (2010) conducted an experimental investigation on the structural behavior of concrete filled thin walled steel tubular stub column with tab stiffeners. The stiffening was achieved by welding together four pieces of lipped angle with two parts of the lips were notched and folded vertically in order to form internal tab stiffeners. The effects of the tab stiffeners on the bond and compressive strengths were concluded using 18 and 10 specimens respectively. It was observed that the tab stiffener improved both the bond strength and the axial load capacity of the CFST short column tested. Krishan *et al.* (2016) offered an algorithm and computer program using theoretical failure loads for concrete filled steel tube elements to calculate their capacity. Hua *et al.* (2014) conducted experimental

study on thirty nine specimens. Discussed parameters are ratio between width of steel tube and thickness, concrete strength, presence of ribs, and arrangement of concrete reinforcing bars. As a result, strength, durability and rigidity are improved. AL-Eliwi *et al.* (2017) compared lightweight Aggregate Concrete Filled Steel Tube columns with Self-Compacted Concrete Filled Steel Tube (SCCFST) columns under axial loading. Four different L/D ratios and three D/t ratios were used in the experimental program to delve into the compression behaviours. While with the SCCFST specimens the global buckling governed the failure mode of long specimens without any loss in capacity. Considering a wide range of column geometries (short, medium and long columns), this paper extends the current knowledge in composite construction by examining the potential of two promising and innovative structural concrete types in CFST applications.

Most of previous researches, conducted on circular CFST columns did not take into consideration effect of H/D ratios in the design equations. Thus, CFST columns use in practice is rare because design provisions among codes vary significantly. Moreover, available design equations for sections with ring stiffeners need to be verified for all H/D ratios. Accordingly, the current research aims to study experimentally the behavior and design of stiffened CFST columns. The test specimens were chosen to widen the experimental investigation through including D/t effect in addition to method of load application i.e. steel only, concrete only or composite. Other studied parameters are global slenderness ratio i.e., H/D and presence of external stiffeners. Thus, twenty seven specimens are tested to determine the impact of those parameters. Load capacities, vertical deflections, vertical strains and horizontal strains are all recorded for every specimen.

## 2. General

In order to analyze the behavior of CFST columns subjected to concentric load, specimens were tested experimentally. All specimens consisted of a circular steel section fabricated from cold formed galvanized steel plates longitudinally welded with electric resistance welding. The outer diameter of pipes was 127 mm. Various test specimens



Fig. 1 Various specimens

Table 1 Limits of maximum D/t ratio for composite sections

Code	Local slenderness ratio D/t (Eq. code)	Max
ACI-318 Specifications		
ECP 205-2001(ASD)	$(8E_s^* / f_y)^{0.5}$	67.42
ECP 205-2007(LRFD)		
ECP 203-2007		
EC4	$90*(235/ f_y)^{0.5}$	73.54
AIJ	$1.5 \times 23500 / f_y$	100.14

\*Where:  $E_s$  (Modulus of elasticity of steel) =  $2.1 \times 10^5$  MPa and  $f_y$  (Yield strength of steel) = 352 MP

Table 2 Specimen symbols definition

Load application	S	Steel load
	C	Composite load
Specimens height	40	400 mm
	100	1000 mm
Steel pipe thickness	200	2000 mm
	2	2 mm
Additional parameter and distribution	4	4 mm
	H	Hollow Steel Section
Steel pipe thickness	St	St (add stiffener)
	No	No. (number of stiffener on specimens)

are shown in Fig. 1 where D/t ratios are equal to 63.5 i.e., class 4 and 31.75 i.e., class 1 according to EC4 for steel hollow sections. Different codes set a limit for the maximum D/t ratio for composite sections to avoid local buckling, as shown in Table 1.

2.1 Studied parameters

The specimen’s names defined with symbols were divided to letters and numbers according to load application, specimen height, steel pipe thickness, additional parameter and additional parameter distribution along the specimen length respectively as shown in Table 2.

In order to study the effect of using ring stiffeners on the results, two main groups of specimens were prepared; each group consisted of several specimens. Control specimens had different H/D ratio as shown in Table 3. Specimens’ lengths were 400 mm, 1000 mm and 2000 mm which corresponded to H/D ratios 3.14 (short columns), 7.874 (medium columns) and 15.748 (long columns) respectively according to classification of AIJ. Six specimens of steel tubes with pipe without any concrete filling were used as control specimens with D/T equals to 63.5 and 31.75, respectively. Specimens with D/T equal to 63.5 and 31.75 respectively consisted of six specimens, which were filled with concrete and loaded on both the concrete core and the steel pipe. Specimens with D/T ratio equal to 63.5 consisted of sections filled with concrete and loaded through the steel

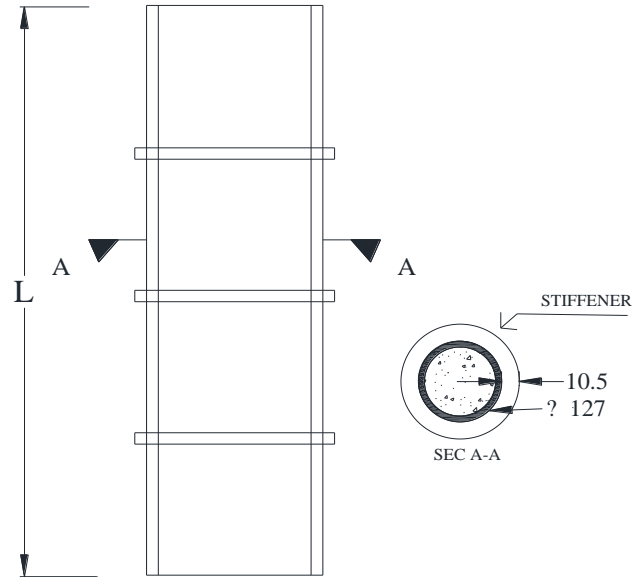


Fig. 2 Cross sections of stiffened specimens



Fig. 3 Steel tubes after filling with concrete

shell.

All stiffeners used in stiffened specimens were square cross sections 10.5 mm × 10.5 mm as shown in Fig. 2. Specimens with D/T ratios equal to 63.5 and 31.75, respectively consisted of six specimens, the sections were filled with concrete and loaded through the concrete core and the steel pipe. Stiffeners distribution along the length of the specimen is shown in Table 3. Specimens with D/T ratio of 63.5 consisted of three specimens who were filled with concrete and loaded through the concrete core and the steel pipe. Specimens with D/T ratio equal to 63.5 consisted of sections filled with concrete and loaded through the steel shell.

2.2 Specimens construction methodology

Fabrication of the steel parts at the workshop included using electric saw to cut of the steel pipe to the required sizes, then executing all fillet weld lines for stiffeners. Finally, the steel specimens were painted with rust inhibitor.

Table 3 Details of specimens

Specimen code	t (mm)	D/t	H (mm)	H / D	Concrete infill	Load application	Stiffener distribution along the specimen length	Ultimate koad (kN)	Failure mode
S40-2-only			400	3.14			-	255	Local
S100-2-only	2	63.5	1000	7.87	None	Steel	-	230	Local
S200-2-only			2000	15.75			-	220	Global
S40-4-only			400	3.14			-	608	Local
S100-4-only	4	31.8	1000	7.87	None	Steel	-	580	Global
S200-4-only			2000	15.75			-	520	Global
C40-2			400	3.14			-	860	Yield
C100-2	2	63.5	1000	7.87	Filled	Composite	-	743	Global
C200-2			2000	15.75			-	724	Global
S40-2			400	3.14			-	830	Yield
S100-2	2	63.5	1000	7.87	Filled	Steel	-	716	Local
S200-2			2000	15.75			-	713	Local
C40-4			400	3.14			-	1260	Yield
C100-4	4	31.8	1000	7.87	Filled	Composite	-	1098	Global
C200-4			2000	15.75			-	1078	Global
C40-2-St1			400	3.14			0.5 H	958	Yield
C100-2-St3	2	63.5	1000	7.87	Filled	Composite	0.25 H	816	Global
C200-2-St3			2000	15.75			0.25 H	802	Global
C40-2-St2			400	3.14			0.33 H	1075	Yield
C100-2-St5	2	63.5	1000	7.87	Filled	Composite	0.167 H	830	Global
C200-2-St7			2000	15.75			0.125 H	802	Combined
S40-2-St2			400	3.14			0.33 H	999	Yield
S100-2-St5	2	63.5	1000	7.87	Filled	Steel	0.167 H	882	Global
S200-2-St7			2000	15.75			0.125 H	780	Global
C40-4-St1			400	3.14			0.5 H	1295	Yield
C100-4-St3	4	31.8	1000	7.87	Filled	Composite	0.25 H	1179	Global
C200-4-St3			2000	15.75			0.25 H	1052	Global

After that, the fabricated parts were transported to Ready-Mix concrete mixing plant where mixing of 1.5 m<sup>3</sup> of concrete took place. Then, pouring of concrete mixture in the steel tube from the top as illustrated in Fig. 3 at the same time using concrete vibrator to ensure homogeneity of the mix. Followed by, flattening of the concrete surface at ends of the test specimens after concrete hardening. Testing was carried out at the laboratory of the faculty of engineering in Mattaria- Helwan University. To facilitate load application, pipes are filled with concrete except 10 mm from both ends.

### 2.3 Test set-up

The frame consisted mainly of horizontal I-beam fixed to two vertical column I-beams by bolts. The I-beam column was rested on the floor. The load was applied using load cell of capacity of 2×103 kN. Electrical pump was used, and 5 LVDT were used to measure the vertical deformation and the horizontal deflection at mid height. The columns were vertically positioned and the upper and lower ends were hinged at a strong frame. The upper end of column was laterally supported by elastic anchors just to

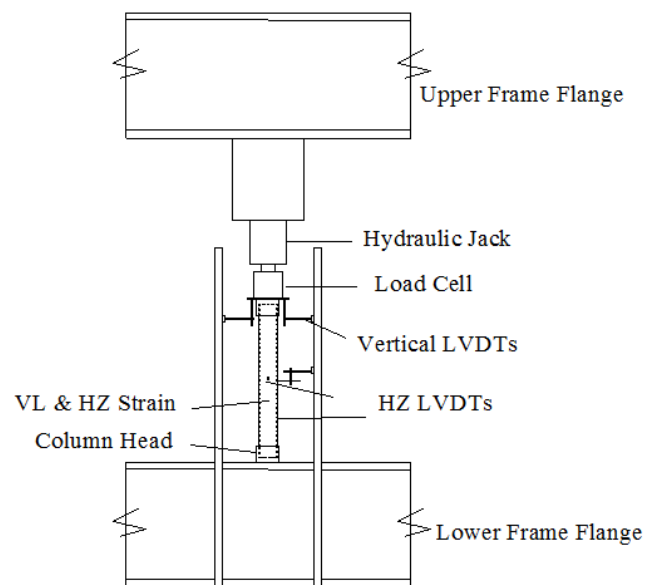


Fig. 4 Test setup for specimens

prevent the drop of specimens during test as shown in Fig. 4.

The load was applied using load cell of capacity of  $2 \times 103$  kN. Electrical pump was used, and 5 LVDT were used to measure the vertical deformation and the horizontal deflection at mid height. The columns were vertically positioned and the upper and lower ends were hinged at a strong frame. The upper end of column was laterally supported by elastic anchors just to prevent the drop of specimens during test.

#### 2.4 Instrumentation and Data Acquisition System

One of those instruments was the load cell which was used as an indicator of the applied load. It was placed between the top end of the specimen and the top end bearing of the testing machine. The strains in the vertical and the circumferential directions for outer steel tubes were measured electrically using strain gauges. Two electrical strain gauges were used for steel. The strain gauges were installed in perpendicular directions at the middle part of the outer steel tube with special care.

Five Linear Variation Displacement Transducers (LVDT) of length 100 mm each was placed at two different locations on the outer surface of the steel tube in order to measure the vertical and horizontal overall deformation of the column at various load levels up to failure. (LVDT 1) and (LVDT 2) were used to monitor the vertical movement of column. (LVDT 3) and (LVDT 4) were used to monitor horizontal movement of the column wall at mid height and (LVDT 5) was used only for specimens with height equal 2000 mm to measure the horizontal deformation at quarter height from the top. All test data was controlled by a data acquisition system as shown in Fig. 5.

#### 2.5 Materials properties

This section described the properties of various materials used in the experimental program, steel and concrete. In order to determine the mechanical properties of the steel tube, tensile coupon tests were conducted to determine the stress-strain characteristics as tensile yield strength and elastic modulus.

Test coupons prepared in accordance with DIN 50125 (2016) were conducted to establish the constitutive properties of the welded steel pipes used in this test program. It was identical to the known stress-strain curve of steel material. The results of the tests showed that the steel yield strength,  $F_y$ , was 352 MPa and  $F_u$  was 418 MPa. The modulus of elasticity of all steel,  $E_s$ , was  $2 \times 105$  MPa.

The properties of concrete were determined by standard concrete cubes from each batch by the mean compressive strength and elasticity modulus of the used concrete. Dimensions of the standard cubes were  $150 \times 150 \times 150$  mm and those of standard cylinders were 150 mm diameter and 300 mm height. Six concrete test cubes were cast at the same time with the specimens. Three of them were tested under compression after 7 days and three were tested after 28 days. The average cube strength after 7 and 28 days were 35.5 MPa and 42 MPa, respectively. Three cylinders were tested under compression after 7 days and three were tested



Fig. 5 Instrumentation and Data Acquisition System



Fig. 6 Local Failure for specimen with steel only (short and medium columns)

after 28 days. The average cylinder strength after 7 and 28 days were 28.3 MPa and 32.1 MPa, respectively.

### 3. Results and discussions

#### 3.1 Failure mechanism

First, specimens that were not filled with concrete, local buckling failure were observed in the steel short and medium tubes as shown in Fig. 6. Meanwhile, global



Fig. 7 Global Failure for specimen with steel only (long columns)



Fig. 8 Yielding Failure for specimen C40-2-St2



Fig. 9 Global Failure for specimen C100-2-St5



Fig. 10 Combined Failure for specimen C200-2-St7

buckling occurred due to increase in the specimen height and/or  $D/t$  ratio as shown in Fig. 7. Second, specimens filled with concrete and loaded on concrete, yielding or global buckling modes of failure occurred based on the specimen height as shown in Figs. 8 and 9 respectively. Meanwhile, Fig. 10 showed combination between yielding at early stages of loading followed by global buckling. It is worth to mention that increasing the ratio of  $D/t$  did not affect the failure mode because dimensions were chosen according to limits set by codes to prevent local buckling. Finally, it can be noticed that both the presence and distribution of stiffeners had no effect on the mode of failure.

### 3.2 Behavior of concrete filled tubes

The effect of various parameters on the behavior of CFST columns is discussed accompanied with load versus vertical deformation, longitudinal strain and hoop strain of different specimens.

#### 3.2.1 Effect of height to diameter ( $H/D$ ) ratio

First, behavior of short columns is discussed, which included: ultimate load versus vertical displacement, longitudinal strain, hoop strains for both cases unstiffened and stiffened specimens. All specimen results showed that vertical displacement increased as the ratio  $H/D$  increased. This is attributed to the decreases in the specimen stiffness according Hook's law. Therefore, the vertical deformation is

directly proportional with the specimen height. Specimens in Fig. 11 behaved as empty steel column at the initial loading due to the absence of concrete at the top and bottom parts. This explains the decrease of load resistance for the first time due to pipe local buckling. After 18 mm of vertical deformation, the loading plates of the testing machine come in contact with the concrete which start to contribute directly to the load carrying capacity. This increase in load carrying capacity continued until the ultimate strength of the concrete was reached where the maximum vertical displacement was equal to 29.9 mm. Stiffened specimens had elastic high slope line before yielding. Then, the slope decreased due to stiffness reduction. The increase in vertical deformation at the same load for increasing H/D ratio resulted from the decreases of the specimen stiffness due with increase in height controlled by Hook's law. The vertical deformation was directly proportional with the specimen height. The vertical deformations recorded maximum value of 9.925 mm.

By increasing load value, the longitudinal strain in steel wall increased. Firstly, the relationship for all specimens had a linear behavior up to yield strain value ( $\epsilon_y = 0.0018$ ),

then it became non-linear until the ultimate load was reached. The longitudinal tensile strain of short column (S40-2) recorded 0.003883 at  $P_y$  of steel and it increased without any increase in the load until the loading plates of the testing machine come in contact with the concrete. After that point, the increase in load value caused an increase in the longitudinal strain until strain value of 0.0109 at load 670 kN. Then, the strain decreased until the ultimate load. That may be due to the failure stage which leads to break up the strain gauge and loss its function as shown in Fig. 12.

Hoop tensile strain values measured in short column (S40-2) were the highest compared to other specimens as shown in Fig. 13. The hoop tensile strain value measured in that column recorded 0.00347 at  $P_y$  of steel without any increase in the load until the loading plates of the testing machine come in contact with the concrete. Since, the steel tube expands and exceeds the yield strain in the radial direction due to compressive loads in its longitudinal direction. For the other specimens, additional tensile strains resulted from circumferential steel hoop tensile developed to provide lateral confining pressure to the concrete without reaching yield strain. The load strain relations for the tested specimens are almost similar in shape until the load reached  $0.8P_u$ . A linear behavior in the early stages of loading is observed with small strain values. Then, the strain values increase non-linearly with loading until failure. Otherwise, increasing the load value caused an increase in the

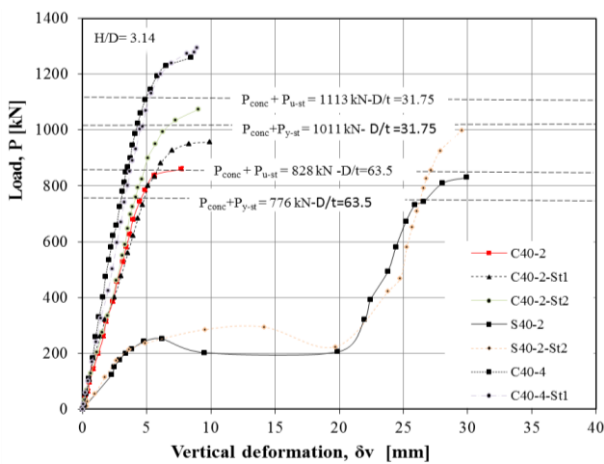


Fig. 11 Load-Vertical deformation curves of specimens with  $H/D = 3.14$

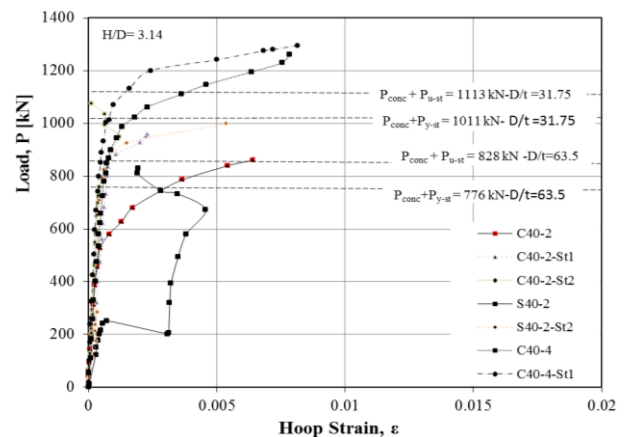


Fig. 13 Load-Hoop strains curves of specimens with  $H/D = 3.14$

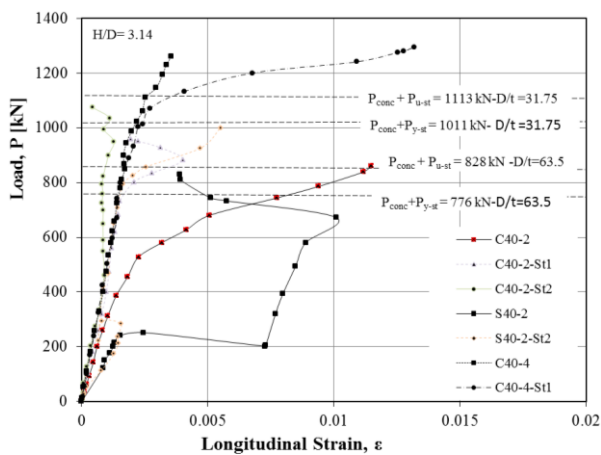


Fig. 12 Load-Longitudinal strains curves of specimens with  $H/D = 3.14$

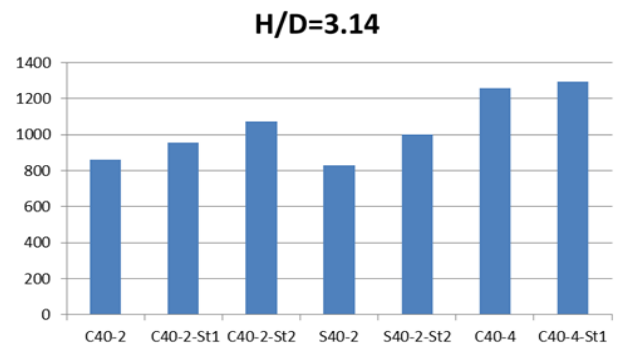


Fig. 14 Ultimate loads for specimens with  $H/D=3.14$

longitudinal strain until strain value of 0.004562 at load 670 kN. Then, the strain decreased until the ultimate load, which may be due to the failure stage which led to break up the strain gauge and losing its function. Ultimate load values of specimens are shown in Fig. 14 for specimens with H/D equal to 3.14. It is obvious that stiffened specimens showed slightly higher compressive strength than unstiffened. In addition to the role of steel wall thickness which enhances clearly the ultimate load values.

Second, specimens with medium length, load versus vertical deformations is plotted in Fig. 15. Maximum value was recorded in specimen C100-2 and is equal to 32.7 mm. Firstly, elastic high slope line appears prior to yielding. Then, the slope is reduced due to stiffness reduction. The vertical deformation is directly proportional with the specimen height. The highest value of all specimens is for specimen S100-2. As shown in Fig. 16, longitudinal strain versus load relationship for all specimens had a linear behavior up to yield strain value followed by nonlinear behavior until reaching the ultimate load. The observed longitudinal strains at peak load are 0.001804 for specimen C100-2-St3. The observed hoop strains values at peak load were 0.001151 which is less than short column specimen (S40-2) as shown in Fig. 17. Lateral confining pressure to

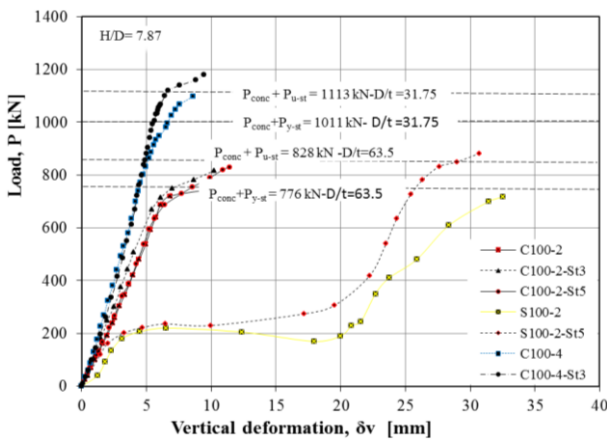


Fig. 15 Load-Vertical deformation curves of specimens with H/D = 7.87

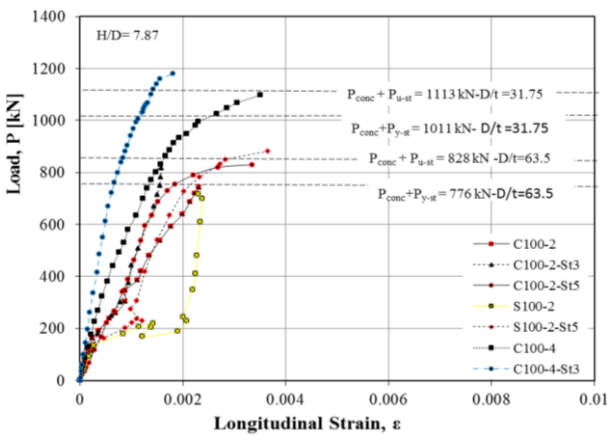


Fig. 16 Load-Longitudinal strains curves of specimens with H/D = 7.87

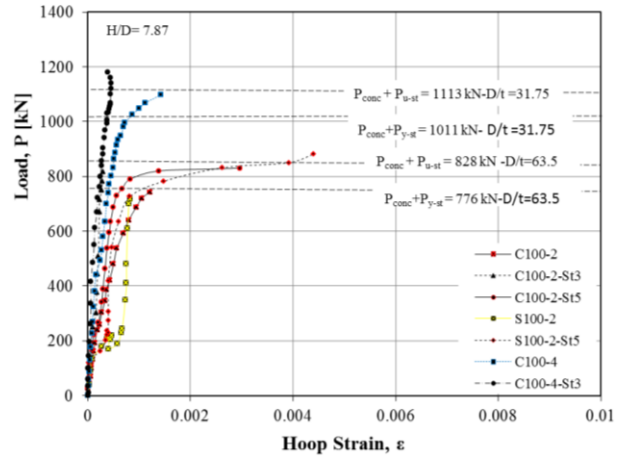


Fig. 17 Load-Hoop strains curves of specimens with H/D = 7.87

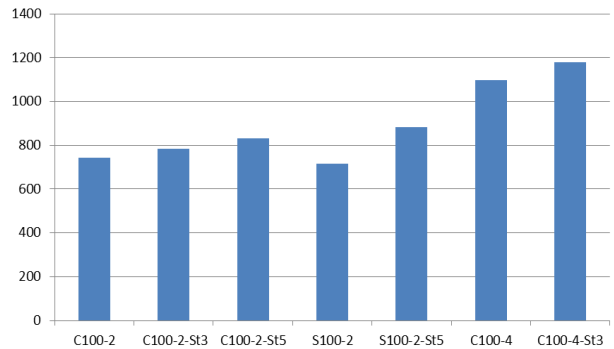


Fig. 18 Ultimate loads for specimens with H/D = 7.87

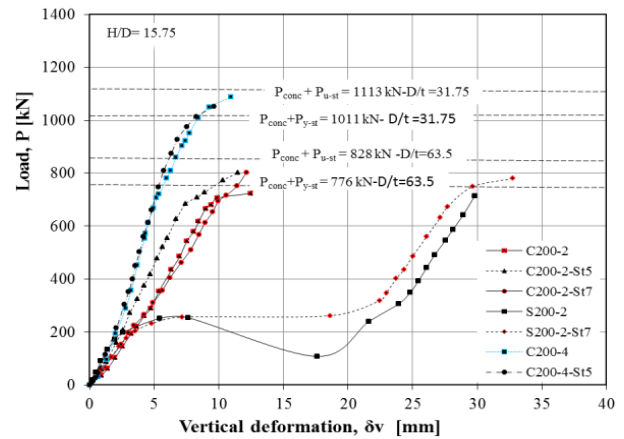


Fig. 19 Load-Vertical deformation curves of specimens with H/D = 15.75

the concrete decreases when compared to wall height. The load strain relations for the tested specimens were almost similar in shape until the load reached  $0.8P_u$ . Regarding ultimate load in Fig. 18, the highest value was specimen C100-4-St3, which is achieved for thicker steel column walls and stiffened specimens.

Finally, long specimens with maximum vertical displacement equal to 34 mm for specimen S200-2, is shown in Fig. 19, specimen length is directly proportional

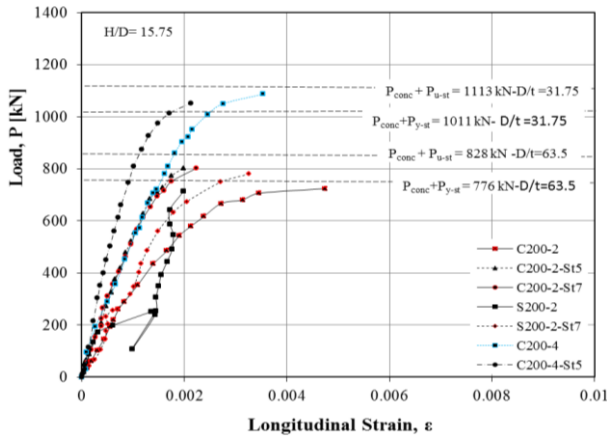


Fig. 20 Load- Longitudinal strains curves of specimens with H/D = 15.75

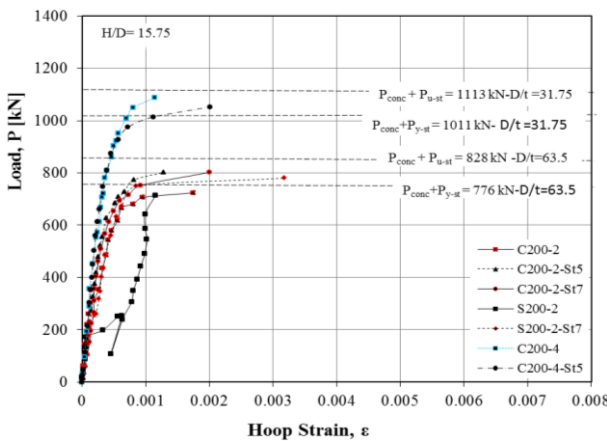


Fig. 21 Load-Hoop strains curves of specimens with H/D = 15.75

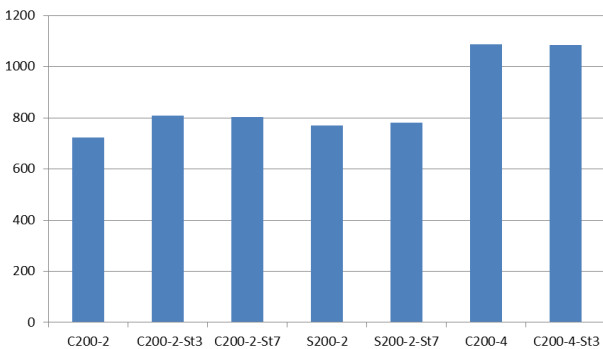


Fig. 22 Ultimate loads for specimens with H/D = 15.75

to vertical displacement. The observed longitudinal strains at mid height of specimens at peak load are 0.001984 for specimen (S200-2), as shown in Fig. 20. Highest hoop strain is observed for specimen S200-2-St7, meanwhile, highest ultimate load is recorded by specimen C200-4 according to Figs. 21 and 22. Presence of stiffener in specimen C200-4 raises its capacity more than other specimens especially stiffened ones. On the other hand, stiffened specimens showed lower hoop strain because of

the redistribution of stresses between specimen steel wall and stiffener.

### 3.2.2 Effect of diameter to thickness (D/t) ratio

The effect of (D/t) ratio on ultimate load of CFST columns is discussed in this section. By increasing the tube thickness, the ultimate load increased. It is seen that, the vertical deformation increased along with increase in load values. Elastic high slope line appears before yielding and buckling. Then, the slope decreases due to reduction in stiffness. For constant H/D ratio at the same load, it's found that increasing D/t ratio leads to increase in vertical deformation. That increase is due to the increase in steel cross section, along with the column confinement and stiffness (Hook's law) as shown in Figs. 14, 18 and 22. Decreasing D/t ratio from 63.50 to 31.75, increased the ultimate load values by 48% for different H/D ratios. Also, the ultimate vertical deformations were almost the same with decreasing D/t ratios for different H/D ratios. In case of specimens with ratios H/D equal to 3.14 and D/t of 63.50, the presence of stiffeners only increased the ultimate load by 11.4% and 25% for 0.5 H and 0.25 H spacing, respectively.

From Figs. 12, 16 and 20 it was observed that, by increasing load values, the longitudinal strain in steel wall increased. First, the relationship for all specimens had a linear behavior up to yield strain value ( $\epsilon_y = 0.0018$ ), then it became non-linear until the ultimate load. For constant H/D at the same load, it was found that, increasing D/t ratio leads to an increase in the longitudinal strains.

Figs. 13, 17 and 21 showed the variation in the axial load versus the hoop strains which was measured at the mid height of steel tubes for the tested specimens. The load strain relations for the tested specimens were almost similar in shape until the load reached 350 kN. The ultimate hoop strains were almost the same with decreasing D/t ratios for different H/D ratios. A linear behavior in the early stages of loading was observed with small strain values, and then the strain values increased non-linearly with the loading till failure.

### 3.2.3 Effect of ring stiffeners

A comparison is conducted between control and stiffened specimens to study the effect of adding and distributing stiffeners to CFST columns. First, as for specimens with H/D ratio equal to 3.14, when D/t ratio was equal to 63.50 and load application was on composite section, it was found that, adding stiffeners increased the ultimate loads values by 11.4% and 25% for stiffener distribution 0.5 H and 0.25 H, respectively. Also, significant enhancement in load capacity equal to 20% was observed in specimens with load application on steel only and with 0.25 H stiffeners distribution. It was noticed that at early loading stages, steel wall in composite specimens dilated more than concrete so no full bond was achieved which weakened strength and stiffness of specimens. Whereas, adding stiffeners had a slight increase i.e., 3% in ultimate loads of specimens with 0.5 H stiffeners distribution, D/t ratio equal to 31.75 and load application on composite section. Axial load versus vertical deformations indicated that, the behavior of all specimens was similar up to the certain

values of  $P_{conc.} + P_{u-st.}$  for both D/t ratios and load applications. It was observed that the presence of stiffeners increased the vertical deformation that was corresponding to the increase in the ultimate loads values.

When D/t ratio was equal to 63.5 and composite section was loaded, it was found that the presence of stiffeners caused hoop yield strain to occur at 0.85 of the ultimate load. Stiffeners also, delayed longitudinal yield strain corresponding to the ultimate load. The recorded delay was from 55% to 90% of the ultimate load values for 0.5 H stiffeners distribution. Otherwise, the strain didn't reach yielding of the tested specimens. Also, the yield strain occurred at 80% of the ultimate load when load application was on steel. Thus, presence of stiffeners delayed the yield strain value corresponding to the ultimate load.

Second, when H/D ratio is equal to 7.87, the values of ultimate loads of specimens in group A and B showed that increased ultimate load percentages were 5.4% and 12% for 0.5 H and 0.25 H, respectively. Also, acceptable enhancement in load capacity was observed in specimens with load application on steel only with improvement of 20% for 0.25 H. As well as adding stiffeners increased the ultimate load value by 7% for 0.5 H at D/t of 31.75 with load application on composite section. Overall, vertical deformations for all other specimens increased at ultimate load. Hoop strain reached yield strain at 0.9 of the ultimate load value. Regarding, longitudinal strain of all specimens, it was found that the presence of stiffeners delayed yield strain corresponding to the ultimate load. Meanwhile, in case of D/t ratio equal to 31.75 the strain of the tested specimen reached yield strain at ultimate load.

Third, when H/D ratio is equal to 15.75, adding stiffeners increased the ultimate loads and the corresponding vertical deformations by 11% for both 0.5 H and 0.25 H in specimens with D/t ratio equal to 63.50 and load application on composite section. On the other hand, ring stiffeners had a slight effect on both ultimate loads and vertical deformation for the other cases. Presence of stiffeners caused hoop strain to reach yield at 0.9 of the ultimate load value and it delayed longitudinal yield strain corresponding to the ultimate load.

#### 4. Design equations

An analytical model was proposed by Lai and Ho (2014) to predict axial capacity of confined and unconfined columns. This model calculates total capacity of columns by summation of individual components of steel and concrete.

Von mises yield criterion of steel tube

$$\sigma_{S\theta}^2 + \sigma_{S\theta}\sigma_{SZ} + \sigma_{SZ}^2 = \sigma_{Sy}^2 \quad (1)$$

$$N = \sigma_{SZ}A_{St} + f_{CC}A_C \quad (2)$$

$$A_{St} = A_s + \frac{\pi}{4}d^2 \frac{\pi D f_{yr}}{S \sigma_{sy}} \quad (3)$$

$$f_{CC} = f'_C + K f_r \quad (4)$$

Table 4 Verification of analytical model results ( $N_{eq}$ ) with test results ( $N_{test}$ )

Specimen	$N_{test}$ (kN)	$N_{eq}$ (kN)	$N_{eq}/N_{test}$
C40-2	860	701.74	0.82
C40-2-St1	958	763.43	0.80
C40-2-St2	1075	824.70	0.77
C40-4	1260.00	1073.81	0.85
C40-4-St1	1295.00	1133.54	0.88
C100-2	743.00	701.74	0.94
C100-2-St3	783.00	775.40	0.99
C100-2-St5	830.00	824.51	0.99
C100-4	1098.00	1073.81	0.98
C100-4-St3	1179.00	1145.06	0.97
C200-2	724	701.74	0.97
C200-2-St3	809	753.66	0.93
C200-2-St7	802	800.41	1.00
C200-4	1087	1073.81	0.99
C200-4-St3	1052	1123.32	1.07

Where

$\sigma_{SZ}$  is axial stress in steel tube

$\sigma_{S\theta}$  is hoop stress in steel tube under biaxial state

$\sigma_{Sy}$  is uniaxial yield strength in steel tube

$A_{St}$  is total area of steel including area of rings

$A_C$  is concrete cross section area =  $D-2t$

$\sigma_{sy}$  is uniaxial yield strength of steel tube

$f_{yr}$  is yield strength of steel rings

$f_{CC}$  is confined concrete

$f'_C$  is unconfined concrete cylindrical strength

$f_r$  is confining pressure

$K = 4.1$

Verification of this design model ( $N_{eq}$ ) as shown in Table 4 was conducted on specimens studied in this research ( $N_{test}$ ) and good agreement of results was observed for medium and long columns. On the other hand, short columns showed variation in their test results when compared to analytical model by up 23%. Thus, it can be seen that analytical model underestimates ultimate loads of short columns. The role of stiffeners is not effective in short columns especially class 1 since failure occurs by yielding. Therefore, when yield load of short columns was compared with test results, results were acceptable with maximum variation of results by up to 11%.

#### 5. Conclusions

This paper discusses concrete filled tubes. The main purpose of this discussion is to determine the factors which affect their behavior. Studied parameters are H/D ratio, D/t ratio and using stiffeners. Experimental work including twenty seven specimens is carried out and here are the main conclusions:

- Two failure modes are observed: yielding or global. For short columns, the thin-wall of steel fails under yielding stress. Meanwhile, for long columns failure is due to global buckling.
- D/t ratio is inversely proportional to ultimate load values, by increasing the tube thickness ultimate load increases. For example, by decreasing D/t ratios from 63.50 to 31.75, ultimate load increases by 48% at the same values of H/D ratios.
- In case of short columns with class 4 sections, presence of stiffeners increases ultimate load by 11.4% and 25% for large and small stiffener distribution along specimen length, respectively. On the other hand, short columns with class 1 sections, presence of stiffeners slightly increases ultimate load by (2-4) %.
- Long columns with H/D equals to 15.75 with class 4 sections, presence of stiffeners increases the ultimate load by 6.0% and 12% for large and small stiffener distribution along specimen length, respectively.
- Adding stiffeners to medium columns with H/D equals to 7.87 and with class 1 sections, increases the ultimate load by 7%. Meanwhile, columns with class 4 sections show an increase equal to 12% for both large and small stiffeners distribution.
- As for long columns with H/D equals to 15.75 and with class 1 sections, no change in the ultimate load is noticed in presence of stiffeners.
- All concrete filled tubes develop tensile hoop due to the development of circumferential steel hoop tension to provide lateral confining pressure for the concrete.

## References

ACI Committee 318, (1999), Building code requirements for reinforced concrete, (ACI 318-99) and commentary (ACI 318R-99). Detroit: American Concrete Institute.

AIJ (1997), Recommendations for design and construction of concrete filled steel tubular structures, Architectural Institute of Japan, Tokyo, Japan.

AISC (2005), Specification for Structural Steel Buildings, ANSI/AISC 360, American Institute of Steel Construction, Chicago, IL, USA.

Ajel, H.A. and Abbas, A.M. (2015), "Experimental and analytical investigations of composite stub columns", *Int. J. Innov. Res. Sci. Eng. Technol.*, **4**(2).

AL-Eliwi, B.J., Ekmekyapar, T., Faraj, R.H., Gogus, M.T. and AL-Shaar, A.A. (2017), "Performance of lightweight aggregate and self-compacted concrete-filled steel tube columns", *Steel Compos. Struct., Int. J.*, **25**(3), 299-314. <https://doi.org/10.12989/scs.2017.25.3.299>

BS 5400 (1979), Steel, concrete and composite bridges: Part: 5 Code of practice for design of composite bridges, London, British Standards Institution.

BS EN Eurocode 4 (1994), Design of Composite Steel and Concrete Structures, General rules and rules for buildings.

DIN 50125 (2016), Testing of metallic materials - Tensile test pieces.

EN 1993-1-4 (2006), Eurocode 3: Design of Steel Structures, Part 1-4: General rules, Supplementary rules for stainless steel, European Committee for Standardization CEN, Europe.

Fam, A., Qie, F.S. and Rizkalla, S. (2004), "Concrete-filled steel tubes subjected to axial compression and lateral cyclic loads", *J. Struct. Eng.*, **130**(4), 631-640. [https://doi.org/10.1061/\(ASCE\)0733-9445\(2004\)130:4\(631\)](https://doi.org/10.1061/(ASCE)0733-9445(2004)130:4(631))

Gupta, P.K., Sarda, S.M. and Kumar, M.S. (2007), "Experimental and computational study of concrete filled steel tubular columns under axial loads", *J. Constr. Steel Res.*, **63**, 182-193. <https://doi.org/10.1016/j.jcsr.2006.04.004>

Hajar, J.F. (2000), "Concrete-filled steel tube columns under earthquake loads", *J. Progress Struct. Eng.*, **2**, 72-81. [https://doi.org/10.1002/\(SICI\)1528-2716\(200001/03\)2:1<72::AID-PSE9>3.0.CO;2-E](https://doi.org/10.1002/(SICI)1528-2716(200001/03)2:1<72::AID-PSE9>3.0.CO;2-E)

Hajjar, J.F., Molodan, A. and Schiller, P.H. (1998), "A distributed plasticity model for cyclic analysis of concrete-filled steel tube beam-columns and composite frames", *Eng. Struct.*, **20**(4-6), 398-412. [https://doi.org/10.1016/S0141-0296\(97\)00020-5](https://doi.org/10.1016/S0141-0296(97)00020-5)

Hu, H.T., Huang, C.S., Wu, M.H. and Wu, Y.M. (2003), "Nonlinear analysis of axially loaded concrete-filled tube columns with confinement effect", *J. Struct. Eng.*, **129**(10), 1322-1329. [https://doi.org/10.1061/\(ASCE\)0733-9445\(2003\)129:10\(1322\)](https://doi.org/10.1061/(ASCE)0733-9445(2003)129:10(1322))

Hua, W., Wang, H.J. and Hasegawa, A. (2014), "Experimental study on reinforced concrete filled circular steel tubular columns", *Steel Compos. Struct., Int. J.*, **17**(4), 517-533. <https://doi.org/10.12989/scs.2014.17.4.517>

Krishan, A.L., Troshkina, E.A. and Chernyshova, E.P. (2016), "Efficient design of concrete filled steel tube columns", *Procedia Eng.*, **150**, 1709-1714. <https://doi.org/10.1016/j.proeng.2016.07.159>

Lai, M.H. and Ho, J.C.M. (2014), "Behaviour of uni-axially loaded concrete-filled-steel-tube columns confined by external rings ", *Struct. Des. Tall Special Build.*, **23**(6), 403-426. <https://doi.org/10.1002/tal.1046>

Nishiyama, I. and Morino, S. (2004), "Summary of research on concrete-filled structural steel tube column system carried out under the US-Japan cooperative research program on composite and hybrid structures", ISSN 0453-4972. Paper Number 147.

Patel, V.I. (2013), "Nonlinear inelastic analysis of concrete-filled steel tubular slender beam-columns", Ph.D. Thesis; Department of Civil Engineering, College of Engineering, University of Victoria, Melbourne, Australia.

Petrus, C., Hamid, H.A., Ibrahim, A. and Parke, G. (2010), "Experimental behaviour of concrete filled thin walled steel tubes with tab stiffeners", *J. Constr. Steel Res.*, **66**(7), 915-922. <https://doi.org/10.1016/j.jcsr.2010.02.006>

Sakino, K., Nakahara, H., Morino, S. and Nishiyama, I. (2004), "Behavior of centrally loaded concrete-filled steel-tube short columns", *J. Eng. Struct.*, **2**, 180-188. [https://doi.org/10.1061/\(ASCE\)0733-9445\(2004\)130:2\(180\)](https://doi.org/10.1061/(ASCE)0733-9445(2004)130:2(180))

CC